Supporting Information

Single-molecule localization microscopy with the Fluorescence-Activating and absorption-Shifting Tag (FAST) system

Elizabeth M. Smith[†], Arnaud Gautier[#], and Elias M. Puchner[*,†].

[†]School of Physics and Astronomy, University of Minnesota, Minneapolis, MN 55455

[#] PASTEUR, Département de Chimie, École Normale Supérieure, PSL University, Sorbonne Université, CNRS, 75005 Paris, France

Table of Contents

Supplemental figures

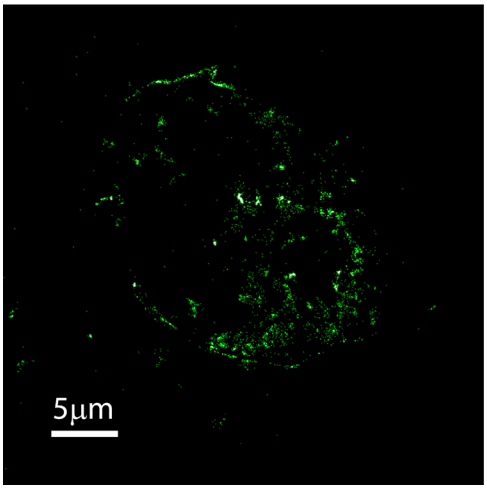

Figure S1. Super-resolution image of mitochondria
Rendered super- resolution image of MTS-FAST:HBR 3-5DOM in mitochondria (97pM HBR 3-5DOM, 6515 frames). The same U2OS cell is shown in the conventional fluorescence image in Figure 1A.

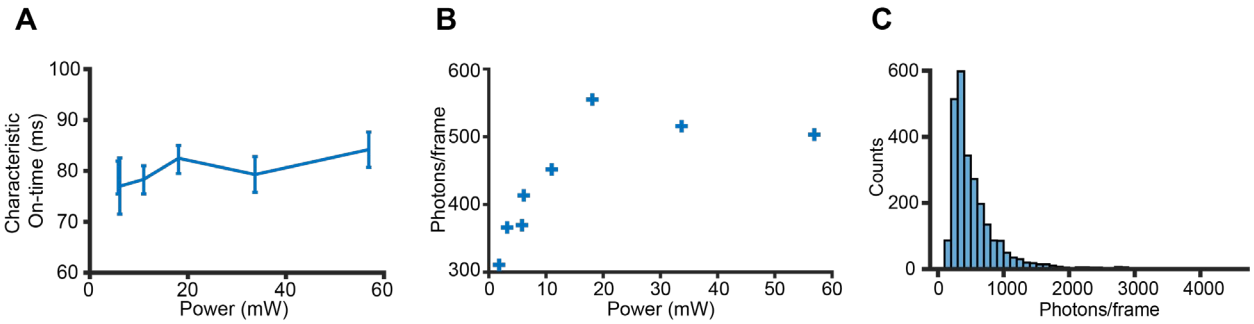

Figure S2. Photophysical characterization and optimization of FAST:HBR-3,5 DOM
(A) The characteristic fluorogen on-times (example plot and fit shown in Figure 2C) are stable over a revelant range 561 laser powers. Error bars signify 95% confidence intervals in fitting. (B) Photon counts for different 561 nm laser power indicating a max photon number of 550 photons/frame at 18mW (power density ~1kW/cm^2). (C) The distribution photon counts detected from single FAST-fluorogen complexes at 18mW.

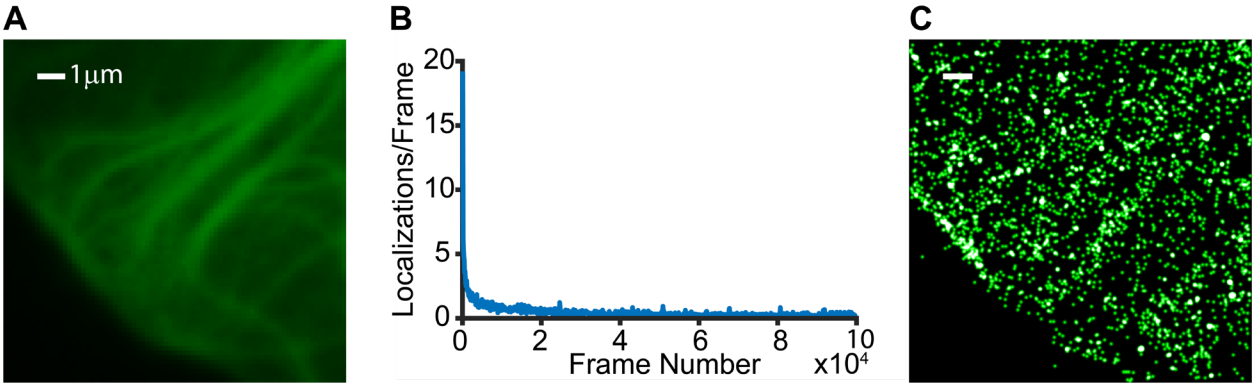

Figure S3. Ensconsin-FAST:HBR-3,5DOM in fixed U2OS cells in PBS.
(A) Conventional fluorescence image of microtubules (320 nM fluorogen, average 50 frames) confirms specific labeling and proper expression levels of Ensconsin-FAST. (B) The localization density (localizations/frame) significantly decreased over the data acquisition time. (C) Photo-destruction of the FAST:fluorogen complex hindered the construction of a high quality super-resolution fluorescence image (10 nM fluorogen, 100,000 frames).

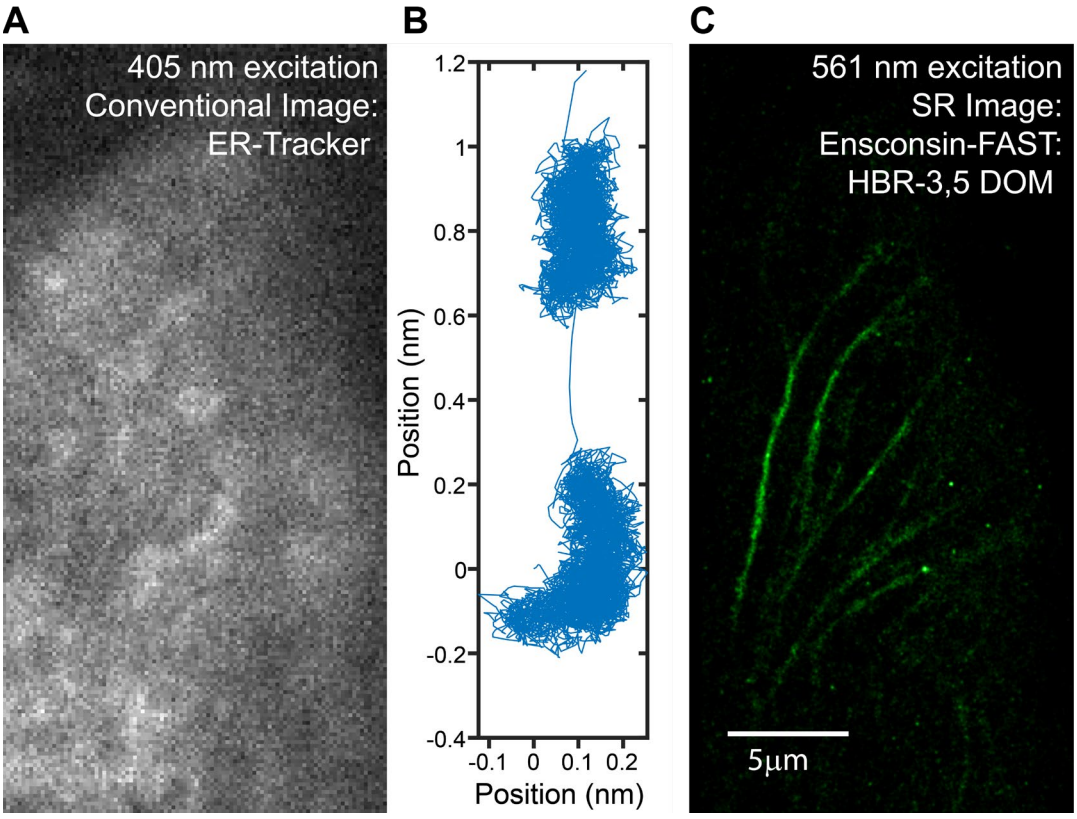

Figures S4. ER-Tracker Blue-White DPX for drift correction
ER-Tracker Blue-White DPX is used in combination with Ensconsin-FAST:HBR-3,5DOM to perform SMLM in fixed U2OS cells. The conventional fluorescence image from the ER-Tracker (A) is used determine the cell sample drift (B) and correct for drift in the rendered SR image (C).

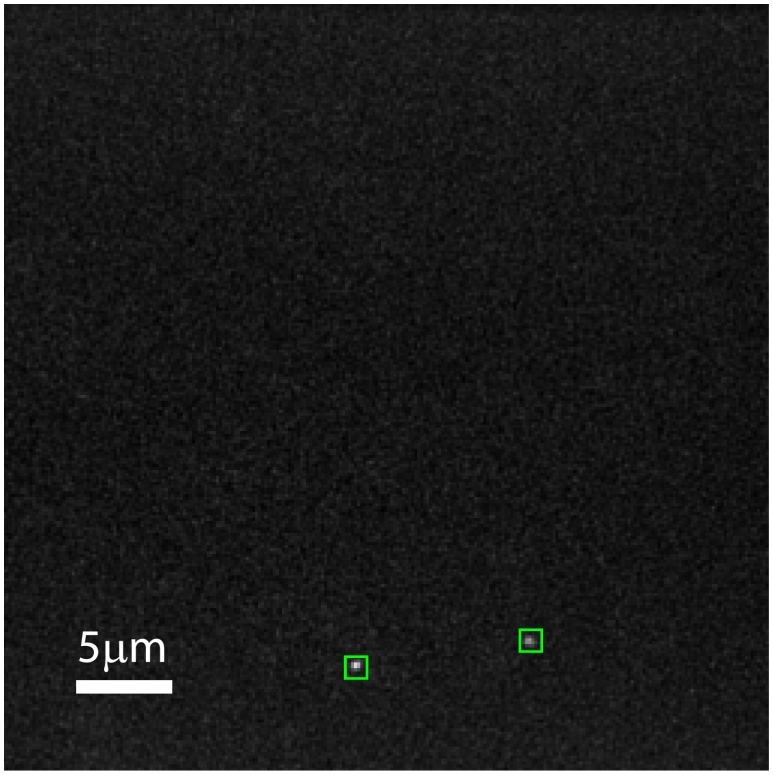

Movie S1. Raw MTS-FAST:HBR-3,5DOM data
Individual frame of the raw data. The movie is 1200 representative frames of MTS-FAST:HBR 3-5DOM in fixed U2OS cells which play at 5fps (acquisition speed, 20Hz). The specific activation of fluorescence allows FAST:fluorogen emitters to be precisely fit and localized over all the frames.

MATERIALS and METHODS

Sample Preparation

All studies were performed using transiently transfected ATCC U2OS cells that were a kind gift from Dr. Jochen Mueller (University of Minnesota). Cells were maintained in DMEM medium (Gibco) with 10% fetal bovine serum, and were subcultered in eight-well coverglass chamber slides (Nunc, ThermoFischer) 12 hours before transfection. Transient transfections were carried out using GeneJET (ThemoFisher), according the manufacturer's instructions, 12-24 hours prior to the measurements. Immediately before measurement, the growth medium was replaced with Dulbecco's phosphate-buffered saline (PBS) with calcium and magnesium (Gibco). For fixation, cells were treated with 4% formaldehyde in PBS for 15 minutes at room temperature and then were washed three times in PBS. The cells shown in Figure 3 were treated with 100nM of ER-Tracker Blue-White DPX (Molecular Probes) for drift correction according to the manufacturer's instructions prior to fixation.

The cloning of the Ensconsin-FAST (microtubule-binding protein) and MTS-FAST (mitochondria targeting sequence) plasmids for mammalian cell expression have been previously described.[1,2]

Addition of Fluorogen dyes and GOC

Stock solutions of HMBR and HBR-3,5 DOM were prepared at a concentration of 20 mM in DMSO and stored at -20°C. HBR-3,5 DOM was further diluted and added to well at various concentrations prior to measurement. For the typical protein expression levels in the experiments, micromolar concentrations of the fluorogen resulted in conventional bulk fluorescence, whereas picomolar to low nanomolar concentrations produced a sparse localization density appropriate for single-molecule localization microscopy. For most experiments (except Figure 1F-J and Figure 2E), a fluorogen concentration that resulted in conventional bulk fluorescence was used to select cells and then the overall concentration was diluted for SR imaging with PBS buffer. Alternatively, for the experiment shown in Figure 2E, 100pM of HBR-3,5 DOM was mixed with 25nM of HMBR (green-yellow fluorogen analog, Ex/Em 488/493–797 nm) before adding the fluorogens to the well. Cells were selected for measurement using the bulk fluorescence signal from HMBR in the green channel and no dilution was needed prior to super-resolution imaging of HBR-3,5 DOM in the red channel. For the experiment shown in Figure 3, glucose oxidase and catalase (GOC) was added to the well just prior to SR imaging at concentrations of 7.1 U ml^{-1} of glucose oxidase (Aspergillus niger, EMD Millipore), 1 kU ml^{-1} of Catalase (Aspergillus niger, EMD Millipore), and 4g L^{-1} of glucose.

Experimental Setup and Data Acquisition

Super-resolution microscopy experiments were performed on a custom-built microscope as previously described.[3] The microscope is based on a Nikon Ti-E inverted microscope with the Perfect Focus System. Three solid state activation/imaging lasers (OBIS 405-100-CW, OBIS 488-50-CW, OBIS 561-100-CW; Coherent) are combined using dichroic mirrors, aligned, expanded, and focused to the back focal plane of the oil objective (100 Apo TIRF N.A. 1.49; Nikon). The lasers are controlled directly by the computer. A quad-band dichroic mirror (zt405/488/561/640rpc, Chroma) separates the fluorescence emission from the excitation light. The fluorescence emission light was subsequently split by a 562nm beam splitter (T562 lpxr, Chroma) into long (red, >562nm) and short (green, <562nm) wavelength channels and filtered by emission bandpass filters (ET595/50 and ET525/50, Chroma). The two channels were

simultaneously recorded at a frame rate of 20 Hz with an electron multiplying CCD camera (iXon+ DU897U-CS0-#BV; Andor). The camera was cooled down to −68 °C and the amplifying gain was set to 30. To estimate the used power density for the activation and excitation laser, we measured the power of the laser at the objective lens and divided it by the illuminated area. The 561-nm laser powers at the objective ranged from 0.1-1 mW (~6-62W/cm^2) for conventional fluorescence imaging and from 15-18 mW (power density ~1kW/cm^2) for SR imaging. During image acquisition, the axial drift of the microscope stage was stabilized by the Perfect Focus System.

Imaging sequences and powers were varied based on the fluorogen concentration, the cell preparation conditions (fixed versus live), and the experiment. For the experiments shown in Figure 1A-D, Figure 2, Supplementary Figure 1A, the 561-nm excitation laser was continuously applied at the power density mentioned above. For Figure 1F-J, data was recorded with a laser shutter sequence comprising four frames of 561 nm excitation for super-resolution imaging followed by one frame of 488 nm excitation to decrease the fluorescence localization density. The power of the 488 nm laser started at ~10mW and was decreased over time to maintain an optimum localization density (Figure 1G, orange). The SMLM data shown in Figure 3 Figure S3, and Figure S4 was recorded with a laser shutter sequence comprising nine frames of 561-nm excitation for SR imaging followed by one frame of 405-nm excitation (power: 23 μW, density ~1W/cm^2) to produce a conventional fluorescence image of the ER-Tracker for sample drift correction. A representative signal from the ER-Tracker is shown in Figure S4A. Both data acquisition and analysis were performed using custom-written software.

Basic Image Analysis

A typical SR image was generated from a sequence of 50,000–100,000 image frames, recorded at 20 Hz. For each imaging frame, fluorescent spots were identified and fit to an elliptical Gaussian function to determine their centroid positions, intensities, widths, and ellipticities using INSIGHT software (Zhuang lab, Harvard). Based on these parameters, peaks too dim, too wide, or too elliptical to yield satisfactory localization accuracy were rejected from further analysis. For all localizations the fit parameters such as the x and y coordinates, photon number, background photons, and frame of appearance were saved in a list for further analysis. Besides the number of photons detected from each molecule, another factor that limits the localization accuracy was sample drift during the course of the experiment. By correlating the fluorescently labeled ER images recorded in each 10th frame and by tracking the centroid of the correlation function, the sample drift was determined and subtracted from the x and y coordinates of all localizations. For image presentation, each localization point was rendered as a normalized 2D Gaussian peak.

Localizations belonging to the same FAST protein will create a spatial signature (radial distribution function, RDF) that defines the uncertainty in position determination and thus the underlying experimental resolution of the system.[3–6] The pair correlation function (PCF), the distributions of distances between any pair of two localization, was calculated in MATLAB by creating a histogram (H) from the distances between localizations N and by dividing each bin by N and the area at the distance r_i:

$$PCF(r_i) = \frac{H(r_i)}{N \times (\pi(r_i + \Delta r)^2 - r_i^2)}$$

where H_i is bin i of the histogram, r_i is the distance of bin i, and Δr is the bin width. The experimental resolution of the FAST:fluorogen system was determined by fitting the PCF with a 2D Gaussian function whose sigma is represents as the uncertainty in position determination. The resolution profiles in Figure 3 were constructed by adding up the localizations within a defined region and projecting them either onto the x-axis (single localization) or along the axis of the microtubule.

For single molecule diffusion analysis, traces were generated by linking localizations in consecutive frames that appear within a distance of 2 μm. For each single-molecule trajectory (n>150) longer than three consecutive frames, the mean-square displacement (MSD) was calculated by averaging the displacement of all time intervals with length delta t in a custom-written Igor-Pro program. The diffusion coefficient was calculated by linear fitting of MSD vs lag-time curve and using the 2D linear diffusion equation: $\left\langle r^2 \right\rangle = 4DT$. The shaded band surrounding the MSD vs time curve represents a standard error of the mean displacements from the multiple traces.

REFERENCES:

(1) Plamont, M.-A., Billon-Denis, E., Maurin, S., Gauron, C., Pimenta, F. M., Specht, C. G., Shi, J., Quérard, J., Pan, B., Rossignol, J., Moncoq, K., Morellet, N., Volovitch, M., Lescop, E., Chen, Y., Triller, A., Vriz, S., Le Saux, T., Jullien, L., and Gautier, A. (2016) Small fluorescence-activating and absorption-shifting tag for tunable protein imaging in vivo. *Proc. Natl. Acad. Sci. U. S. A. 113*, 497–502.

(2) Li, C., Plamont, M.-A., Sladitschek, H. L., Rodrigues, V., Aujard, I., Neveu, P., Le Saux, T., Jullien, L., and Gautier, A. (2017) Dynamic multicolor protein labeling in living cells. *Chem. Sci. 8*, 5598–5605.

(3) Puchner, E. M., Walter, J. M., Kasper, R., Huang, B., and Lim, W. A. (2013) Counting molecules in single organelles with superresolution microscopy allows tracking of the endosome maturation trajectory. *Proc. Natl. Acad. Sci. U. S. A. 110*, 16015–16020.

(4) Veatch, S. L., Machta, B. B., Shelby, S. A., Chiang, E. N., Holowka, D. A., and Baird, B. A. (2012) Correlation functions quantify super-resolution images and estimate apparent clustering due to over-counting. *PloS One 7*, e31457.

(5) Sengupta, P., Jovanovic-Talisman, T., Skoko, D., Renz, M., Veatch, S. L., and Lippincott-Schwartz, J. (2011) Probing protein heterogeneity in the plasma membrane using PALM and pair correlation analysis. *Nat. Methods 8*, 969–975.

(6) Sengupta, P., Jovanovic-Talisman, T., and Lippincott-Schwartz, J. (2013) Quantifying spatial organization in point-localization superresolution images using pair correlation analysis. *Nat. Protoc. 8*, 345–354.